

<https://doi.org/10.1038/s44432-025-00001-1>

Divergent urban vegetation inequality in Northern and Sunbelt United States cities under climate extreme events

Check for updates

Yu Yan¹, Chunyu Dong¹ , Jie Guo², Zhiyong Liu¹, Kairong Lin¹, Xiaohong Chen¹, Di Long³ & Glen M. MacDonald⁴

Urban vegetation inequality (UVI) undermines the equitable distribution of ecosystem services such as heat mitigation. However, the role of climate variability in shaping UVI remains unclear. Here we have developed a methodology using satellite, census, and climate data to analyze UVI across 245 major U.S. cities. Our study proposed a vegetation polarization index (VPI), calculated as the normalized difference between the 90th and 10th percentiles of NDVI, to measure UVI. We examined how climate events affect UVI differently in the Sunbelt versus northern cities. Sunbelt cities display exacerbated UVI under drought and warmer climates, while colder and wetter conditions may increase UVI in northern cities. Hot droughts can amplify UVI across almost all cities, with Sunbelt cities showing greater vulnerability. We analyzed UVI trends from 2001 to 2020, revealing that Sunbelt cities exhibit worsening UVI trends, while northern cities show improving trends. These changes are related to climate shifts and socioeconomic factors, underscoring the vulnerability of U.S. cities to fluctuating UVI under climate change. Socioeconomic conditions play a significant role in exacerbating this vulnerability.

Urbanization and extreme climate events, such as deadly heatwaves and extreme droughts have caused multiple environmental challenges that impair urban sustainability¹. Urban vegetation as a nature-based solution provides ecosystem services benefits for residents to combat urban climate challenges, e.g., air purification, mitigation of local heat waves, and noise reduction^{2–4}. Through providing these ecosystem benefits, urban green space is strongly associated with reductions in mortality rates by reducing the risk of some dangerous diseases, e.g., cardiovascular disease⁵. The global urban population has grown to 4.2 billion by 2018, accounting for more than half of the total global population⁶. In light of this, governments should consider how to ensure that the majority of urban dwellers can equally receive ecosystem benefits from urban green spaces. This aligns with the United Nations' Sustainable Development Goal 11 (SDG 11)⁷, which aims to make cities and human settlements inclusive, safe, resilient, and sustainable.

Unfortunately, there is considerable evidence that urban vegetation is often unequally distributed among different socioeconomic groups in cities^{8,9}. For example, community greenery is closely linked to the income of residents in many U.S. big cities such as Los Angeles¹⁰. Furthermore, inequality in urban greenness is closely linked to a wide range of socioeconomic and geophysical elements^{10,11}. Disparities in urban greenness

associated with the race and education of residents are more severe than those related to age, income, or household characteristics in cities of northeast U.S. such as New York¹². Serious inequalities in urban vegetation are projected to lead to a disproportionate distribution of ecosystem benefits, including public health gains. This represents a critical environmental justice issue¹³. Thus, a national comparative analysis of urban vegetation inequality across all major U.S. cities ($n = 245$) can provide valuable evidence. Such evidence is needed to monitor and mitigate the negative environmental justice impacts of disparities in vegetation cover and health.

In addition to socioeconomic influences on urban vegetation inequality (UVI), some case studies have shown that global warming and climate extremes are also likely to contribute to this inequality¹⁴. During the exceptional 2012–2016 drought in southern California¹⁵, disadvantaged communities could not afford the rising cost of outdoor water use¹⁶, and thus their vegetation suffered a significant degradation. In addition, although there was no significant relationship between vegetation and income in Phoenix in the 1970s, there was a trend towards an increasing correlation between the two variables by 2000 due to more frequent heatwaves in recent years⁸. Extreme climate events and global warming are a threat to the sustainability of urban vegetation.

¹Center for Water Resources and Environment, School of Civil Engineering, Sun Yat-sen University, Zhuhai, China. ²School of Geography and Planning, Sun Yat-sen University, Guangzhou, China. ³Department of Hydraulic Engineering, Tsinghua University, Beijing, China. ⁴Department of Geography, University of California, Los Angeles, Los Angeles, CA, USA. e-mail: dongchy7@mail.sysu.edu.cn

These studies have primarily examined the effects of climate variability on vegetation health and function. Fewer have explored the relationships between socioeconomic variables and UVI, particularly their dynamics under a changing climate^{17,18}. Urban greenness could be affected by both human activities such as outdoor water usage and climate extremes like droughts. Numerous studies have documented that climate extremes, including heatwaves and droughts, are becoming more frequent and intense under global warming, posing escalating risks to urban ecosystems and populations^{19–21}. Under a global warming scenario of +2 °C, the occurrence of extreme heatwaves is projected to increase by approximately fivefold²², whereas the frequency of droughts is expected to rise nearly threefold²¹. Compound climate events are also expected to intensify²³. Compound climate events are defined as the combination of multiple climate drivers and/or hazards that contribute to societal or environmental risk²⁴. These variations highlight the need to better understand how climate variability and socioeconomic disparities jointly shape urban vegetation inequality.

We therefore ask the following key scientific questions: (1) What are the current state and trends of UVI in U.S. cities? (2) What is the impact of different climate events (i.e., including single and compound climate events) on the city-scale UVI? (3) What cities tend to have higher vegetation inequality trends and why?

To accurately identify the UVI dynamics in the context of global warming, it is important to apply appropriate vegetation greenness indices at the city scale. The Gini Index, a metric originally developed for measuring economic disparities, has recently been applied to quantify urban green inequality²⁵. However, previous studies suggest that the Gini index is more sensitive to changes in the middle-level groups and less sensitive to changes at the top and the bottom of the sample distribution²⁶. Considering the limitations of the Gini Index, here we propose a vegetation polarization index (VPI, see Method), which is derived by calculating the normalized difference between the 90th and 10th percentiles of the Normalized Difference Vegetation Index (NDVI) for a region, to assess UVI dynamics in the continental U.S. cities. The VPI quantifies the disparity between the most and least vegetated areas within a certain region, providing a sensitive measure of extreme vegetation inequality. This is particularly relevant in urban environments, where advantaged socioeconomic groups often have access to greener vegetation, while disadvantaged groups tend to reside in areas with substantially less vegetation. This index enables a more robust assessment of urban vegetation inequality and its response to climatic and socioeconomic factors across U.S. cities.

Results

Divergent distribution of UVI trends

We examined the long-term trends and averages of UVI at the city scale from 2001 to 2020 (Fig. 1). A VPI Z-score trend of >0 indicates an increasing UVI, suggesting that disparities in vegetation greenness between neighborhoods within a city have been widening (see Methods). The study area was categorized into simplified Köppen-Geiger climate zones: arid, snow, warm temperate, and Tropic zones. Our findings reveal that cities in the arid zone exhibit significantly higher UVI levels (VPI = 0.38 to 0.45) compared to cities in the other three climate zones (VPI = 0.27 to 0.32) (Fig. 1a).

Over the past two decades, most cities in southern California and Texas, spanning both temperate and arid zones, have shown a notable increase in UVI (0.003 to 0.008/month). Conversely, cities in the Pacific Northwest, East Coast, and the Great Lakes Region have demonstrated significant declines in UVI (−0.003 to −0.007/month) (Fig. 1b). In total, 46 out of 245 cities experienced an uptick in UVI, with 17 cities showing a statistically significant increase (Supplementary Table 1), primarily concentrated in the arid and temperate zones. Across different climate zones, nearly all cities in the tropic and snow zones exhibited a decrease in UVI. In the temperate zone, 75% of cities and in the arid zone, 56% of cities experienced a similar decline. Notably, cities in the arid zone had the highest proportion (~44%) showing an increasing UVI trend among the four climate zones. In addition, our findings indicate that the average UVI in certain cities within arid zones, such as Phoenix and Las Vegas, has potentially

peaked at its highest level (VPI > 0.34) compared to cities in other climate zones. Moreover, there is an emerging trend of stabilization or even decline in UVI within the arid zone.

Distinctive effects of climate events on UVI between Sunbelt and northern cities

We investigated the impacts of various climate events and their severities on UVI, encompassing both single and compound events such as drought, wet periods, hot droughts, and cold wet episodes. These events were defined based on the 1st and 4th quartiles of monthly drought and temperature indices over the past two decades (Table 1). Different severities of these climate events were identified using various thresholds of these indices during the same period (see Methods). A VPI Z-score greater than 0 indicates that a climate event can exacerbate UVI in a city. The standardized VPI Z-scores enable comparisons across spatial and temporal scales, reflecting the dynamic changes in UVI under different climate events.

The findings indicate a clear disparity in the influence of various climate events on UVI across the Sunbelt and northern U.S. cities. The Sunbelt region comprises 15 southern states in the U.S. and extends from Virginia and Florida in the southeast through Nevada in the southwest, and also includes southern California (typically encompassing the area south of the 36° north latitude parallel)²⁷. Northern cities in this study refer to all major cities located outside the Sunbelt region, primarily in the Midwest, Northeast, and Northwest of the United States. For example, southern California, Texas, and Florida exhibited the highest VPI Z-scores (>0.4) during drought periods, highlighting the exacerbation of UVI in these Sunbelt cities (Fig. 2a). In contrast, during wet periods, UVI in these Sunbelt cities decreased (< −0.2), while it slightly increased in northern cities (>0.1) (Fig. 2b). Additionally, UVI in Texas and California noticeably rose during warmer periods (>0.2), whereas a decline was observed in Florida and northern cities (< −0.1) (Fig. 2c). Strikingly, the spatial pattern of UVI during colder periods was opposite to that during warmer periods (Fig. 2c, d).

Furthermore, the influence of compound climate events on UVI seemed to either amplify or mitigate the effects of individual events, also depending on the geographical locations of the cities. For instance, during warmer drought periods, UVI in the Sunbelt cities was exacerbated compared to a single drought or warm event, whereas northern cities were less affected (Fig. 2e). Notably, hot drought events intensified vegetation inequality across nearly all U.S. cities (Fig. 2g). Additionally, cold wet and colder wet periods resulted in increased VPI Z-scores in northern cities and decreased scores in the south, while warmer drought events exhibited an opposite north-south pattern (Fig. 2e, f, h).

Our findings further highlight the varying impacts of different severities of drought and hot drought on UVI (Supplementary Fig. 1, 2). For instance, during extreme drought periods, all cities exhibited higher VPI Z-scores compared to moderate drought periods (Supplementary Fig. 1). Similar trends were observed across different severities of hot droughts (Supplementary Fig. 2). Interestingly, even mild hot droughts exacerbated vegetation inequality issues in northern cities (Supplementary Fig. 2), whereas only the most severe droughts had a significant impact on northern cities' UVI (Supplementary Fig. 1). This sensitivity suggests that northern cities are more affected by hot droughts than by regular droughts. Furthermore, UVI in northern cities (snow climate zone) showed minimal sensitivity to the severity of droughts, as indicated by VPI Z-scores close to 0 across different drought severities (Supplementary Fig. 1f). However, the severity of hot droughts positively influenced VPI Z-scores across all climate zones, indicating widespread sensitivity of vegetation inequality to hot drought severity (Supplementary Fig. 2e).

We further conducted a comprehensive analysis of VPI Z-scores for the 245 U.S. cities under various single and compound climate events (periods) (Fig. 3). Overall, mean VPI Z-scores were highest during hot drought periods and lowest during wet periods across all cities (Fig. 3b). When analyzed by climate zones, VPI Z-scores peaked in the arid, tropic, and temperate zones during hot drought periods, while reaching their

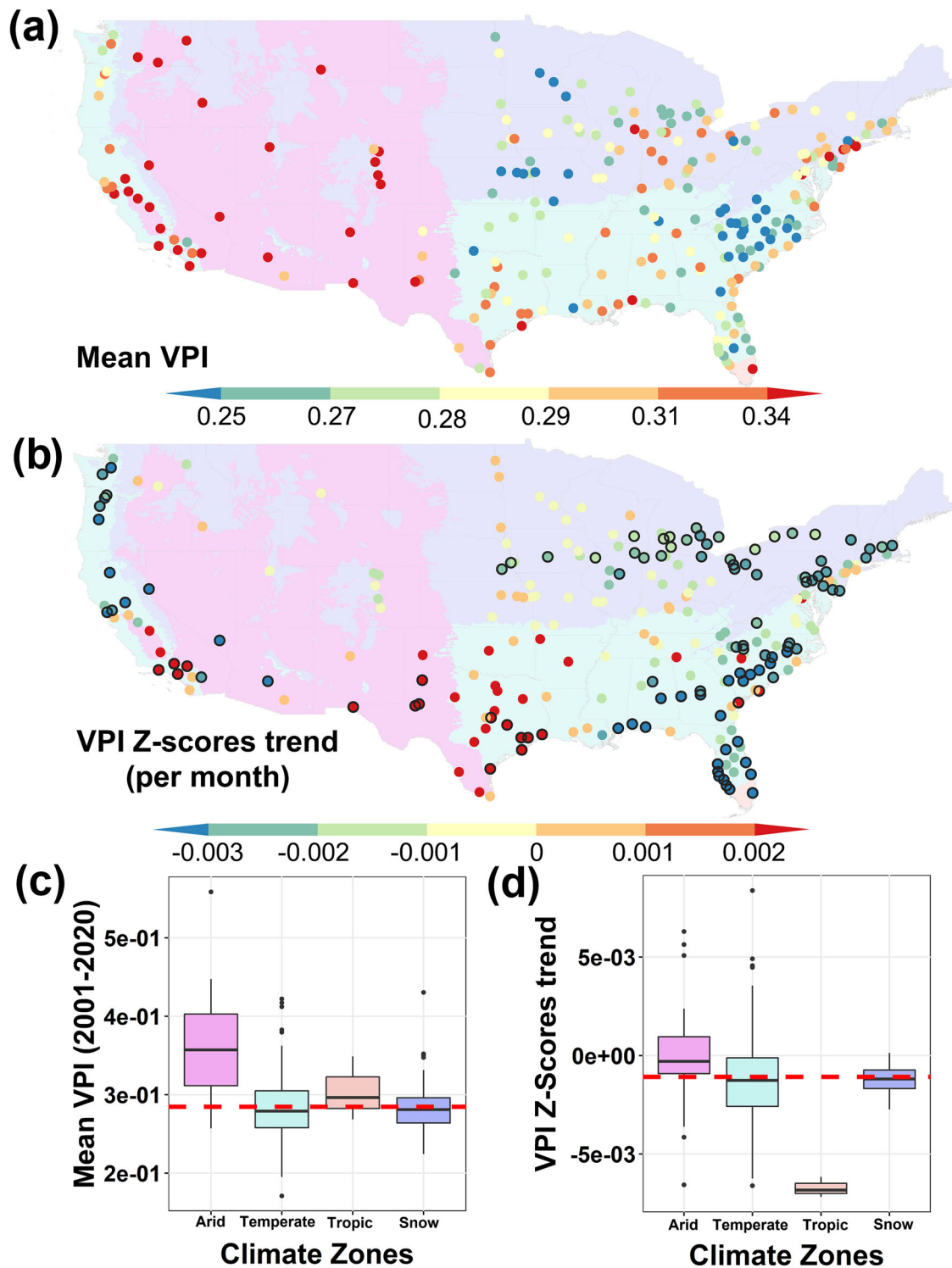


Fig. 1 | The long-term average and trends in UVI. Mean (a) and trends (b) of UVI as represented by VPI for the 245 largest U.S. cities and the respective quartile statistics (c, d) among the four climate zones from 2001 to 2020. Dots outlined in black circles depict statistically significant trends ($p < 0.05$). The red dashed lines indicate the mean values of all 245 cities in the VPI and the trends of VPI Z-scores.

The updated Köppen-Geiger map is used to categorize urbanized areas into four basic climate zones: arid (the western US), snow (the northeastern US), temperate (the southeastern US), and tropic (only in southern Florida) zones. Number of cities in the different climate zones: Arid = 34, Temperate = 122, Tropic = 3, Snow = 86.

highest in the snow climate zone during colder wet periods (Fig. 3a). This highlights hot drought as the most detrimental climate event for UVI across diverse climate zones. Cities in arid, temperate, and tropic zones showed increased UVI during drought or warmer periods, whereas cities in the snow zone experienced elevated UVI during wet or colder climates (Fig. 3a).

Furthermore, hot drought consistently exacerbated UVI irrespective of climatic type or location (Fig. 3a).

Although the mean VPI Z-score of all cities during warmer periods was near zero, the distribution of VPI Z-scores exhibited bimodal peaks (Fig. 3b). Maps of VPI Z-scores during warmer periods revealed distinct UVI

Table 1 | Criteria for defining climate events

Climate Events	Definition
Drought	$SPEI_{90d} < SPEI_{90d-q25}$
Wet	$SPEI_{90d} > SPEI_{90d-q75}$
Warmer	$T_{anom} > T_{anom-q75}$
Colder	$T_{anom} < T_{anom-q25}$
Warmer drought	$(SPEI_{90d} < SPEI_{90d-q25}) \text{ AND } (T_{anom} > T_{anom-q75})$
Colder wet	$(SPEI_{90d} > SPEI_{90d-q75}) \text{ AND } (T_{anom} < T_{anom-q25})$
Hot drought	$(SPEI_{90d} < SPEI_{90d-q25}) \text{ AND } (T > T_{q75})$
Cold wet	$(SPEI_{90d} > SPEI_{90d-q75}) \text{ AND } (T < T_{q25})$

Note: T, T_{anom} and $SPEI_{90d}$ refer to temperature, anomaly temperature, and 90-day SPEI, respectively. q25 and q75 denote the 25th and 75th percentiles of the corresponding variables.

responses between the northern and Sunbelt cities (Fig. 2c). These findings suggest that climate warming may intensify and mitigate UVI in the warmer Sunbelt and the colder northern cities, respectively, indicating differing UVI responses to identical climate events between cities over the two regions.

As the climate continues to warm, the frequency of droughts and heat waves is increasing in many areas, leading to a drier and warmer climate in recent years²⁸. To identify the most vulnerable cities facing increases in UVI during 2001–2020, we calculated the changes in VPI Z-scores (ΔVPI Z-scores) for warm and dry climate periods compared to cold and wet periods (Supplementary Fig. 3). The results showed that ΔVPI Z-scores in the Sunbelt cities climbed significantly as the climate changed from wet/colder/colder wet/cold wet conditions to drought/warmer/warmer drought/hot drought conditions, whereas ΔVPI Z-scores in the northern cities dropped to some extent (Supplementary Fig. 3). Thus, in the drier and warmer future, UVI issues in the Sunbelt cities such as cities in Texas, southern California, Florida, and the southern East Coast may be more noticeable due to their vulnerability to climate change ($p < 0.05$). Meanwhile, the UVI issues in the north-central areas may ameliorate ($p < 0.05$).

Drivers of UVI trends across climate zones

To examine the correlation between long-term climate variable trends and UVI across diverse climate zones (Fig. 4), we employed multiple linear regression (MLR). Since the tropic zone consists of only three cities, the regressions were exclusively conducted for the remaining three climate zones. A rising standardized precipitation evapotranspiration index (SPEI) trend indicates less evaporative demand and often increasing moisture in a region, while a declining trend suggests the opposite. As SPEI includes information on both temperature and moisture, we calculated the variance inflation factors (VIF) of the MLR models, which were all less than 5, indicating weak multicollinearity between predictors (Supplementary Table 2). Furthermore, to facilitate comparisons among variables with varying magnitudes, we standardized the regression coefficients of the different variables. A regression beta value (standardized coefficient) exceeding 0 signifies that the predictor has the potential to exacerbate UVI (i.e., positive effects on VPI trends).

Overall, the results from the four regression models indicate a significant negative association between rapidly moistening climates and UVI trends (Fig. 4). Conversely, rapidly drying climates likely significantly increase UVI trends. Soil climate aridity trends, specifically SPEI trends, emerge as the most critical predictors of UVI trends across all climate zones (Fig. 4). Particularly in arid-climate zones, the climate aridity trend (SPEI trend) shows the strongest coefficient on UVI trends (Fig. 4b). In the temperate zone, increasing aridity in both air (VPD increase) and soil (SPEI decrease) seems to significantly increase UVI trends, whereas climate warming appears to decrease UVI trends (Fig. 4c). In the snow-climate zone, warmer and wetter climate conditions exhibit a negative relationship with UVI trends (Fig. 4d). Additionally, precipitation trends do not show significant effects on altering UVI trends across all climate zones.

We then applied the MLR approach to investigate the city-scale relationship between socioeconomic variables and UVI trends (Fig. 5). The findings indicate that median age exhibited a consistent negative association with UVI trends across all MLR models ($p < 0.05$, Fig. 5). When examined by climate zones, the proportion of Hispanics showed a positive association with UVI trends in the temperate zone ($p < 0.05$, Fig. 5c). In the arid-climate zone, median household income was identified as a negative predictor of UVI trends (Fig. 5b). Conversely, in the snow zone, only median age was negatively predictive of UVI trends (Fig. 5d). Overall, except for the snow-climate zone model, the R^2 values between socioeconomic variables and UVI trends (Fig. 5) exceeded those between climate variables and UVI trends (Fig. 4). This underscores that socioeconomic variables are the predominant predictors of UVI trends. In the subsequent section, we explore potential pathways linking socioeconomic variables to UVI trends.

The MLR analyses of all 245 cities demonstrated a significant influence of five climatic and socioeconomic predictors (Trends in SPEI, temperature, and VPD; Hispanic population, and median age) on UVI trend ($p < 0.05$) (Fig. 4, 5). To compare differences in UVI trends among different percentiles of the five variables, we divided the data into four quantile groups. The 1st quantile group (<Q25) of SPEI trend (decreasing SPEI) showed significantly higher UVI trends compared to the other three quantile groups (Supplementary Fig. 4a). The 4th quantile group (>Q75) of VPD trend exhibited significantly higher UVI trend than the 2nd quantile group (Q25–Q50) (Supplementary Fig. 4b). Warmer climate (3rd and 4th quantiles) resulted in significantly lower UVI trend (Supplementary Fig. 4c). Regarding socioeconomic conditions, the 4th quantile group (>Q75) of Hispanics showed significantly higher UVI trend than the other three groups (Supplementary Fig. 4d). An increase in the median age of the cities significantly decreased UVI trends (Supplementary Fig. 4e).

To uncover non-linear associations between UVI trend and the predictors (all climate and socioeconomic variables), we employed the Random Forest (RF) model and calculated the accumulated local effect (ALE) to elucidate how these predictors impact UVI trends (Supplementary Fig. 5). The analysis reveals that an increase in the median age of individuals within a city, particularly within the range of 35 to 40 years old, is linked with a rapid decrease in UVI trend (Supplementary Fig. 6a). Temperature trends below 0 °C/year exhibit weak relations with UVI trend, whereas temperature trend increases above 0 °C/year are associated with significant declines in UVI trend (Supplementary Fig. 6b), which is consistent with the results of MLR models (Fig. 4), i.e., climate warming likely helps relieve UVI in temperate and snow zones. The growth of cities' Hispanic population ratios between 0–0.6 is positively associated with the UVI trend (Supplementary Fig. 6c). However, higher ratios of the Hispanic population of > 0.7 may negatively predict the UVI trend. Moreover, an increase in the $SPEI_{90d}$ trend below 0 led to rapid declines in the UVI trend, while further increases in the $SPEI_{90d}$ trend over 0 only showed a slight influence (Supplementary Fig. 6d).

Discussion

This study presents a comprehensive investigation of urban vegetation inequality (UVI) through the development of a new Vegetation Polarization Index (VPI), which specifically quantifies extreme disparities in urban green space distribution. By analyzing 245 major U.S. cities at a monthly temporal resolution - an unprecedented approach in UVI research - we provide new insights into the spatiotemporal dynamics of vegetation inequality under climate change (especially under extreme climate events). Our findings indicate that UVI in arid zone cities was significantly higher than in cities of the other three zones (Fig. 1a). This result is consistent with previous studies^{11,29}, which have also linked lower greenness to arid cities. In essence, city-scale UVI demonstrated a significant negative correlation with city-scale greenness. Furthermore, our study revealed an improved equality of urban vegetation among most cities in the past two decades, aligning with existing research (Fig. 1d)³⁰. In contrast to previous annual-based analyses³⁰, our findings based on a monthly time-scale investigation show that UVI in

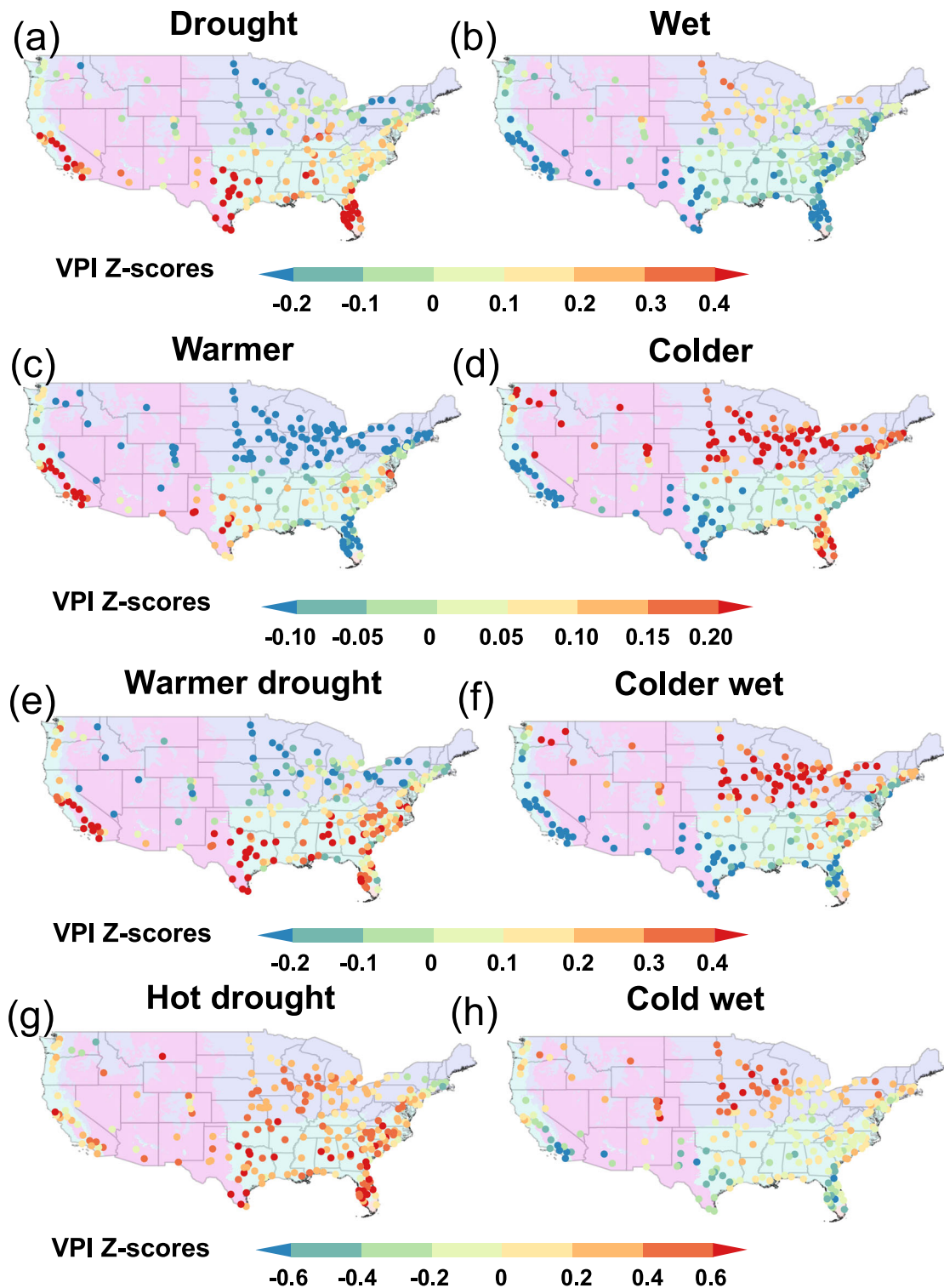


Fig. 2 | The influence of climate events on UVI. VPI Z-scores of the 245 U.S. cities under single and compound climate events: drought (a), wet (b), warmer (c), colder (d), warmer drought (e), colder wet (f), hot drought (g), and cold wet events (h). A VPI Z-score >0 indicates a potential worsening of UVI under specific climate event.

Cities categorized by updated Köppen-Geiger climate zones: arid (dark red), snow (purple), warm temperate (blue), and tropic zones (orange). Note: The tropic zone includes only three cities, potentially limiting its representativeness.

the Sunbelt cities, such as those in Texas and southern California, has significantly increased over the past two decades (Fig. 1b), whereas many northern and eastern cities experienced a slight decrease in UVI (Fig. 1b).

We have also identified key drivers behind these observed UVI trends. Aridification patterns and socioeconomic factors, particularly the proportion of Hispanic residents (positively correlated) and median population age

(negatively correlated), showed significant associations with UVI trends (Fig. 4, 5). Our findings highlight the dynamic nature of UVI variations, which appear to be influenced by both climatic change and socioeconomic conditions. The mechanisms underlying the observed relationships with population demographics (age structure and Hispanic population proportion) remain unclear and warrant further investigation. It is important to

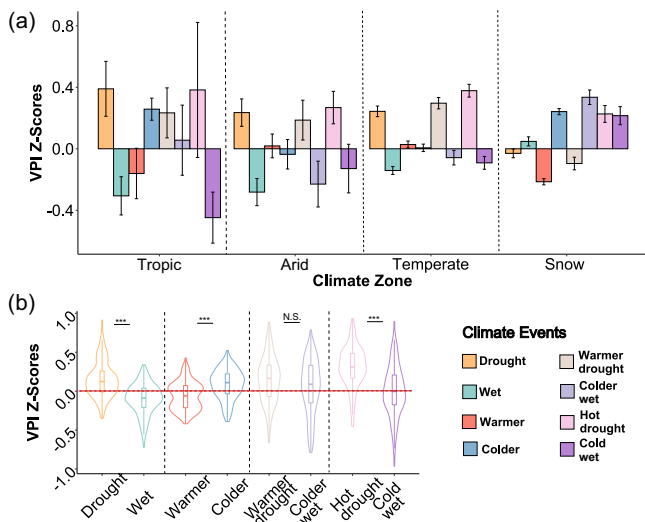


Fig. 3 | The influence of climate events on UVI across climate zones. **a** Bar chart showing mean VPI Z-scores for 245 U.S. cities under different climate events across four Köppen–Geiger climate zones (Tropic, Arid, Temperate, and Snow). Error bars denote approximately 95% confidence intervals. **b** Violin plots illustrating the distribution of VPI Z-scores under each type of climate event, with embedded boxplots indicating quartiles. A positive VPI Z-score (>0) indicates a potential worsening of UVI (i.e., increased vegetation inequality) under the corresponding climate event. Significance levels are denoted as ***: $p < 0.001$ and N.S.: not significant ($p > 0.05$).

note that our regression analyses are predicated on the hypothesis that both socioeconomic changes and climate variability may influence vegetation greenness distribution and temporal patterns. However, the established relationships should not be interpreted as causal without additional evidence, highlighting the need for more comprehensive studies to elucidate these complex interactions.

In addition, temporarily rapid changes in UVI likely also linked to the changing environments, such as extreme climate events. Urban greenery is an ecologically valuable resource with many benefits. However, it tends to be unequally distributed, especially in areas where vegetation is sparse and economic resources are limited. Our findings indicate that under anomalous climatic events such as drought/warming/warm drought, most of the cities in the Sunbelt U.S. displayed intensified UVI, while the northern cities mainly showed increased UVI during colder and wet climate events (Fig. 2, 3). Similar south–north spatial patterns were observed in the effects of drought severities on UVI (Supplementary Fig. 1, 2). Vegetation growth is influenced by changes in radiation, temperature, and precipitation. The magnitude of these effects depends on species composition, climate background, and topography³¹. Such geographic backgrounds can partly explain the different responses of UVI between the Sunbelt and northern cities. In the Sunbelt cities, such as those in Texas and southern California, urban vegetation is typically more limited by water availability and is thus more vulnerable to drought³². In contrast, urban vegetation is more limited by cold temperatures and is less sensitive to drought in the northern cities (snow zones)³³.

Recent studies provide further evidence of the impact of climate events on UVI and highlight the indirect mechanisms through which climate events affect UVI³⁴. In the case of drought periods, there are direct impacts on vegetation physiology that are coupled in some cases by decreased

Fig. 4 | Standardized coefficients for multiple linear regression (MLR) models between trends in climate variables and UVI for different climate zones. The R^2 of the MLR models is presented in the upper left corner. Coefficient values are represented as dots, while bars represent the 95% confidence intervals (CIs), and significant variables are shown in red ($p < 0.05$). ALL: four climate zones (a); Arid: arid zones (b); Tem: temperate zones (c); Snow: snow zones (d).

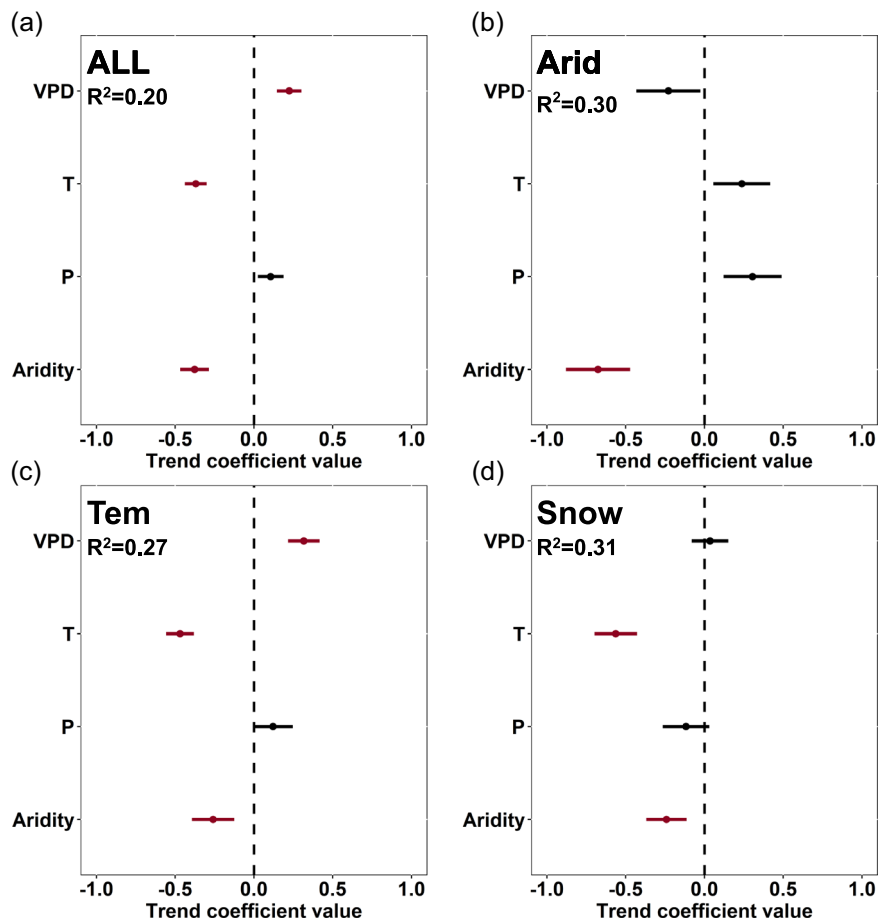
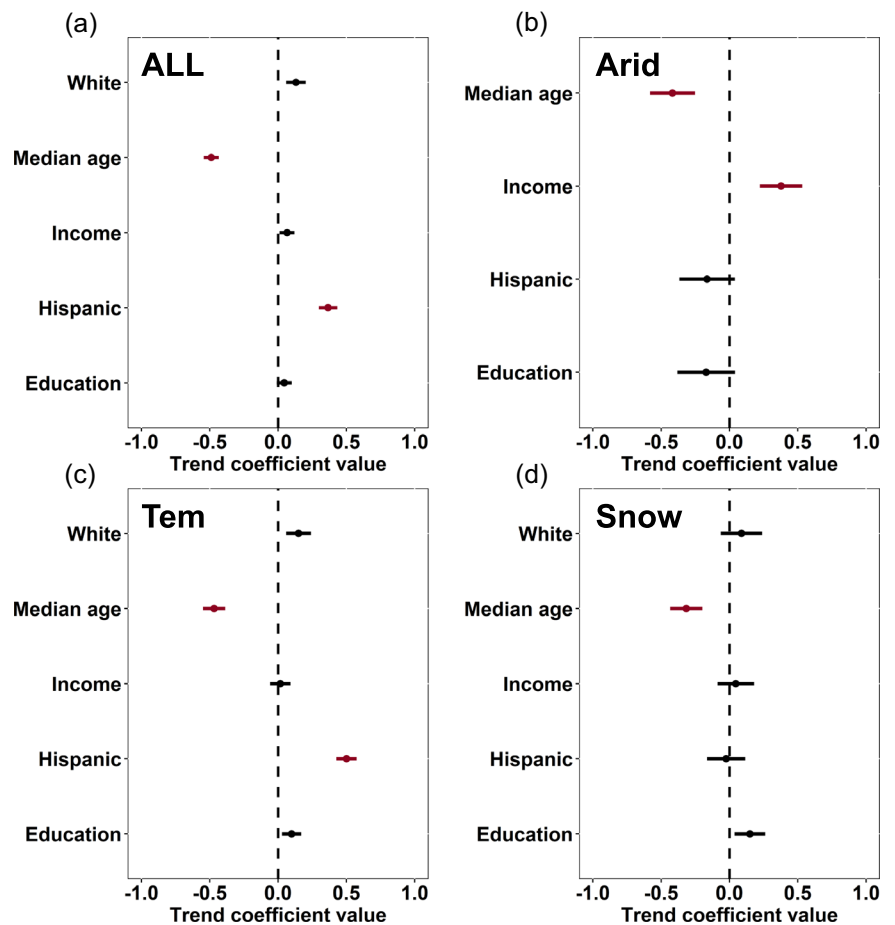


Fig. 5 | Standardized coefficients of MLR models between socioeconomic variables and UVI trends in different climate zones. R^2 of the MLR models is presented in the upper left corner. Regression coefficients are marked as dots, while the bars represent the 95% confidence intervals (CIs), and significant variables are shown in red ($p < 0.05$). In the arid zone, as there was a strong multicollinearity between the Hispanic and White population ($VIF > 5$), we excluded the predictor of the White population based on a stepwise MLR and the Akaike information criterion index (Supplementary Table 3). ALL: four climate zones (a); Arid: arid zones (b); Tem: temperate zones (c); Snow: snow zones (d).



irrigation in response to increasing water costs or restrictions³⁵. Outdoor water usage in areas occupied by economically advantaged groups may not be sensitive to increased water prices, whereas outdoor water usage by economically less well-off groups might significantly decline³⁶. These dynamics can further amplify existing vegetation inequality.

In the case of compound climate events such as hot droughts, most of the cities across the U.S. displayed strong increases in UVI (Fig. 2 and Supplementary Fig. 2). This finding is in line with recent studies³⁷, which suggest that the co-occurrence of high temperatures and drought is particularly harmful to plants. Drought reduces evaporative cooling, thereby intensifying heat stress and causing abrupt declines in plant growth. Previous studies already indicate a negative relation between city-scale greenness and UVI³⁸. Furthermore, the extreme water scarcity due to the compound heat and water stress likely induced intensified UVI in almost all U.S. cities³⁹. This effect is more pronounced in the Sunbelt cities, which are more vulnerable to drought due to higher temperatures and evaporation rates (Supplementary Fig. 2).

Urban vegetation provides key ecosystem services like cooling, flood mitigation, and mental health benefits, which generally increase with greenness. Denser vegetation enhances cooling—critical during heatwaves—while low greenness offers minimal benefits^{39,40}. Previous studies suggest depression risk declines slowly when NDVI is 0–0.4 but drops sharply at 0.4–0.8^{41,42}. Similarly, flood mitigation only improves significantly beyond certain green space thresholds⁴³. Thus, urban planning must address both vegetation inequality and sufficient overall greenness. Our data show most cities have $NDVI_{Q10} < 0.40$ and $NDVI_{Q90} > 0.50$, with a mean difference of 0.22 (Supplementary Fig. 7). This corresponds to daytime LST differences of 1.74 °C (3.03 °C in summer), indicating low-greenness areas receive limited ecosystem benefits. After controlling for elevation and anthropogenic heat,

vegetation cooling effects (CE) were 2–5 times stronger in $NDVI_{Q90}$ areas (-0.3 °C/ +0.1NDVI) than $NDVI_{Q10}$ (-0.05 °C/ +0.1NDVI) (see Method and Supplementary Text 1, Supplementary Fig. 8). Similar patterns emerged in Universal Thermal Climate Index (UTCI^{44,45}) analysis, confirming greenness inequality’s impact on thermal comfort (Supplementary Fig. 9). Ultimately, vegetation inequality translates into disparities in ecosystem service provision, with low-greenness communities receiving disproportionately fewer environmental benefits.

The findings of this study demonstrate widespread, but regionally variable, sensitivity of urban vegetation to climatic factors and the coupling of this with socioeconomic/demographic conditions in the major cities of the United States. It should also be noted that, due to our focus on city-level aggregation, the present study does not address intra-urban (neighborhood-level) variations in vegetation inequality. This limitation may obscure finer-scale disparities and mechanisms that are crucial for understanding environmental justice and equity issues within cities. Future research leveraging higher spatial resolution data and sub-city analyses is needed to provide more insights into local drivers and patterns of urban vegetation inequality. More limitation discussion can be found Supplementary Text 2. The results highlight the urgent need for detailed research and the development of adaptation strategies to protect urban vegetation cover. These strategies should account for the specific vulnerabilities of different regions and socioeconomic or demographic groups to climate change. In the face of climate change, this is critical to ensure an equitable distribution of the benefits of urban vegetation cover. To relieve urban ecological inequality in cities under climate change, it is important to recognize the vulnerability of urban vegetation, implement climate-wise and sustainable landscape planning, and establish sustainable water resource management to maintain vegetation.

Methods

Urban extent

To extrapolate our results to a widespread or national level, this study includes the largest 245 cities in the continental United States (U.S.). The built-up boundaries of these cities were derived from the latest GUB (Global Urban Boundary in 2018) datasets, which were extracted from the high-resolution GAIA (Global Artificial Impervious Area) database (Supplementary Table 4)⁴⁶. The reliable and high-resolution GAIA database jointly uses Landsat series, Sentinel-2, and nightlight satellite products to extract global impervious surfaces. Based on the urban extent thresholds of previous studies^{17,47}, we excluded the cities with a built-up area of less than 100 km², leaving 245 cities as our study area. These cities include various urban socioeconomic conditions, development histories, and climatic characteristics. In this study, “Sunbelt cities” refer to cities located in the following 15 southern U.S. states: Alabama, Arizona, Arkansas, California (southern), Florida, Georgia, Louisiana, Mississippi, Nevada, New Mexico, North Carolina, Oklahoma, South Carolina, Tennessee, and Texas⁴⁸. The “Sunbelt” arises from the region’s high levels of sunshine and warm climate throughout most of the year. All other cities outside these states are classified as “northern cities,” primarily in the Midwest, Northeast, and Northwest of the U.S. In addition, to account for the ecological and climatic heterogeneity across U.S. cities, we also classified cities into climate zones based on the updated Köppen-Geiger climate classification⁴⁹. Each city was assigned to one of four zones (arid, temperate, snow, or tropical) according to its location on the K-G map. The use of Köppen-Geiger zones as a supplementary classification provides a widely recognized climatological framework for analyzing environmental and ecological variation, and has been adopted in recent studies of urban environmental inequality⁵⁰. This dual classification by both region (Sunbelt/northern) and climate zone allows for a more nuanced understanding of how geographic and climatic context shapes urban vegetation inequality.

Demographic and socioeconomic data

The United States Census Bureau provides the 2014–2018 ACS (American Community Survey) 5-year database, which contains both demographic and socioeconomic statistics at the census tract level for these 245 cities in the contiguous United States. Based on previous studies^{10,50}, we collected the socioeconomic characteristics on race, age, and income. These include the median household income in the previous 12 months, the proportion of the white population, the proportion of the Hispanic population, and the median age (Supplementary Table 5). We selected these variables because previous studies have shown that they are closely associated with inequalities in both heat exposure and urban vegetation distribution^{10,39,50}. We excluded the census tracts having a population of 0 and then collected 45,254 census tracts in total for all 245 cities. We further constructed the city-level aggregation of these socioeconomic variables to investigate the association between city-scale UVI and socioeconomic patterns (Supplementary Table 5).

Climate data

Climate variables, including air temperature (T), precipitation (P), vapor pressure deficit (VPD), and standardized precipitation evapotranspiration index (SPEI) at 4 km spatial resolution and 5-day time resolution for the period 2001–2020 were collected from a reanalysis dataset combining both observations and models, i.e., the Gridded Surface Meteorological (GRID-MET) database⁵¹. The SPEI index was applied in this study to characterize the cumulative water balance conditions from the previous 1–24 months (SPEI_{30d}, SPEI_{90d}, SPEI_{180d}, SPEI_{1y}, SPEI_{2y}). The monthly mean SPEI index, temperature, precipitation, and VPD were then calculated for each city by averaging the values of all pixels within that city. Due to the seasonal changes in the climate variables except for the SPEI index (a standardized and normalized index), we calculated the anomalies for these variables⁵². We estimated the trends of those climate variables from 2001–2020 based on the Theil-Sen estimator⁵³.

Vegetation greenness index and Vegetation Polarization Index (VPI)

Normalized Difference Vegetation Index (NDVI) is widely used to estimate the overall vegetation greenness in a given region^{50,54} ($NDVI = (Band_{NIR} - Band_{RED}) / (Band_{NIR} + Band_{RED})$), where $Band_{NIR}$ and $Band_{RED}$ are the surface reflectance in the near-infrared and red bands, respectively). It can assess the local extent and health of urban vegetation, although it cannot directly identify vegetation types (e.g., shrubs, trees, and grasses)⁵⁵. Despite this weakness, the NDVI index is still a widely used remote sensing metric that links vegetation abundance, health, and leaf characteristics⁵⁶. The satellite-based moderate resolution imaging spectroradiometer (MODIS) project provides a global NDVI product (MOD13Q1.006) with a spatial resolution of 250 m and a temporal resolution of 16 days from 2001 to 2020. Here we deliberately excluded data beyond 2020 to eliminate pandemic-induced anomalies, as COVID-19’s wide impacts radically restructured urban economic frameworks and societal interactions in ways that could jeopardize the reliability of the analysis. Besides, areas of water, clouds, heavy aerosols, and cloud shadows have been removed from the database. Then we calculated the pixel-wise monthly mean NDVI values before performing the following analyses.

In this study, the differences in NDVI values among regions in a city are referred to as an urban greenness discrepancy or vegetation inequality. The Gini index has been widely used to measure the inequality of income distribution and natural resource shares⁵⁷. However, the Gini index has been reported to be more sensitive to the middle-level samples and cannot well account for the difference between the highest and lowest levels^{26,58}. In this regard, we further found polarization metrics representing the worst situation of inequality between the highest and lowest levels, referring to the wide gaps in resource or access inequality⁵⁹. The concept of polarization can also be applied to differences in UVI. The World Bank and the Organization for Economic Co-operation and Development have been using the H index (the income share of the top 10% divided by the income share of the bottom 10%, i.e., P90/P10) to measure income inequality or polarization⁶⁰. Moreover, many previous studies have highlighted the importance of measuring the gap between the top 10% and the bottom 10% in quantifying inequality^{26,61}.

Similar to the widely used H index⁶¹, here we also utilized the top and bottom 10% of the monthly mean NDVI in a city to construct a vegetation polarization index (VPI) to reflect the city-level urban vegetation inequality (UVI) as follows (Supplementary Fig. 10 & 11):

$$VPI = \frac{NDVI_{Q90} - NDVI_{Q10}}{NDVI_{Q90} + NDVI_{Q10}} \quad (1)$$

The VPI is calculated by first ranking the NDVI values of all pixels in a city from the lowest to the highest, and then quantifying the normalized difference between the 90th ($NDVI_{Q90}$) and 10th ($NDVI_{Q10}$) percentiles of NDVI values. The advantaged groups have more access to greener vegetation, while the disadvantaged groups have less. VPI can represent the inequality levels of vegetation greenness over a certain region²⁶. Besides, the metrics of percentile dispersion ratios are less sensitive to outliers than other inequality indices, such as the Gini coefficient⁶². The equation for the VPI follows the form of normalized difference spectral indices, and it has many advantages, e.g., simple calculation, easy comparison between different locations, and screening of data noise⁶³.

Previous studies have reported that many disadvantaged groups are mainly clustered in high-density areas and that some advantageous groups with high house values are close to parks or mountains¹⁰. However, the dynamics of the vegetation in parks, mountains, and high-density areas are mainly government-managed and weakly related to the socio-economic state of the community. Hence using P90 and P10 of NDVI to calculate VPI can help exclude this influence on our study.

The main steps to calculate the VPI index and VPI Z-scores using monthly NDVI are summarized as follows:

1. Calculate the monthly mean NDVI for all pixels and identify $NDVI_{Q90}$ and $NDVI_{Q10}$ in each city.
2. Calculate the vegetation polarization index (VPI) based on the $NDVI_{Q90}$ and $NDVI_{Q10}$ values in the city.
3. Calculate the VPI Z-scores (standardized anomalies) to offset the seasonal changes in UVI which is mainly related to plant phenology and vegetation types¹¹.

The variations in VPI Z-scores represent the temporal changes in UVI compared to the long-term baseline (multi-year average). Thus, an increase in VPI Z-scores represents a deterioration in UVI.

Based on the multi-year average NDVI of the 245 U.S. cities, we validated the accuracy of the newly proposed VPI metric against three widely used inequality indices, i.e., Gini Index, Inequality Index, and Wolfson Polarization Index (the equations for three indices in Supplementary Text 3)^{26,64,65}. Traditional inequality metrics, such as the Gini Index, mainly reflect differences among average groups and are less sensitive to the extremes. In contrast, the VPI is specifically designed to capture the gap between the highest and lowest levels of urban vegetation—the “best-off” and “worst-off” areas. This tail sensitivity allows the VPI to detect extreme urban vegetation disparities that might be masked by other indices. Additionally, the VPI’s normalized-difference form makes it robust to differences in absolute NDVI values and allows for direct comparison across cities and time periods. We also validate the correlation between these indices. VPI showed high correlation coefficients with the three inequality indices ($R^2 \geq 0.90$, Supplementary Fig. 12). In addition, we examined the uncertainty of the newly proposed VPI (calculated by the 90th and 10th percentiles) against the other three VPI* indices which estimated by the different percentile combinations ($NDVI_{Q80}$ & $NDVI_{Q20}$, $NDVI_{Q70}$ & $NDVI_{Q30}$, $NDVI_{Q60}$ & $NDVI_{Q40}$). The VPI* index equations were similar to the VPI index. For example, here is the equation for $VPI^*_{(q80-q20)}$:

$$VPI^*(q_{80} - q_{20}) = \frac{NDVI_{Q80} - NDVI_{Q20}}{NDVI_{Q80} + NDVI_{Q20}} \quad (2)$$

The VPI also showed high correlation coefficients with the three VPI* indices by different percentile combinations (e.g., $VPI^*_{(q80-q20)}$, $VPI^*_{(q70-q30)}$, and $VPI^*_{(q60-q40)}$) ($R^2 \geq 0.75$, Supplementary Fig. 13). This is consistent with previous studies suggesting that the gap between the top and bottom 10th percentiles is a good indicator of inequality^{26,29}.

Statistical analyses

We utilized Google Earth Engine (GEE) to pre-process and extract these climate and vegetation datasets and then used R statistical software to build the regression models for investigating the association between the predictors (socioeconomic conditions and climate variability) and the trend in UVI. We performed a quality screening of the data using the reliability bands for each pixel provided by the data source, retaining only those observations that were deemed reliable. Our study focuses on urban vegetation that is heavily influenced by human irrigation and management, such as yard vegetation. Therefore, the National Land Cover Database (NLCD) was used to remove pixels of water, urban areas with high-intensity development, and open spaces such as parks, natural vegetation, soccer fields, and golf courses. It should be noted that natural vegetation within cities can also provide ecosystem services and benefits. However, as this study mainly aims to identify urban vegetation inequality induced by socioeconomic factors, the publicly owned natural vegetation may cause noise information in our analyses and was thus excluded. Meanwhile, we also excluded the pixels with a multi-year average NDVI value of < 0 to ensure that non-vegetation pixels were excluded from the analyses.

In this study, the imbalanced development of urban vegetation is presented as the trend of UVI, obtained by calculating the trend of VPI Z-scores based on the Theil-Sen estimator⁵³. In addition, the Mann-Kendall test method was used to estimate the significance of the UVI trend⁶⁶. As different climatic backgrounds may have an impact on the development of

urban vegetation, we divided the continental United States into four climate zones (arid, snow, warm temperate, and tropical) based on the updated Köppen-Geiger map⁶⁷. Since SPEI data have different time scales, we calculated the correlation coefficients between VPI and SPEI with different time scales for each climate zone. Thus, we selected a specific time series SPEI which showed the highest correlation coefficients with VPI in individual climate zones (Supplementary Table 6).

As suggested by previous studies⁶⁸, multiple linear regression (MLR) mainly captures the linear effects of predictors, while the random forest (RF) model can explore the non-linear effects of variables. To explore the complex impact of socioeconomic conditions and climate variability on UVI, we applied MLR and RF models to quantify the linear and non-linear effects of the eight variables in altering the VPI Z-score trend. We utilized the default $n_{tree} = 500$ for training the random forest model and used the $tuneRF$ function to obtain the best n_{tree} parameter in each model run. The spatial distribution of the main socioeconomic and climate variables was shown in Supplementary Fig. 14 & 15

Meanwhile, we investigated the influence of different climate events on UVI. To identify different climate events, we selected the first and third quartiles as thresholds based on the percentile statistics of temperature, temperature anomalies, and $SPEI_{90d}$ ⁶⁹. The $SPEI_{90d}$ was selected because it shows the highest correlations with VPI for nearly all climate zones (Supplementary Table 6). The criteria for defining different climate events based on percentile thresholds can be found in Table 1.

Here we utilize both temperature (T) and anomaly temperature (T_{anom}) as criteria to identify not only the relatively warmer/colder events compared to the long-term mean climate from 2001 to 2020 but also absolutely hot/cold events that take seasonal climate variability into account. To ensure a larger sample size for each category of climate event given the limited 20 years of records, we refrained from using more extreme temperature thresholds, such as $q20/q80$ or $q10/q90$.

Furthermore, to examine the effect of different severities of drought (or hot drought) on UVI, the drought events were classified into five levels based on the $SPEI_{90d}$ and T. Firstly, drought events were divided into five severities: extreme drought (D_1 , $SPEI_{90d} < -2$), severe drought (D_2 , $-2 < SPEI_{90d} < -1.5$), moderate drought (D_3 , $-1.5 < SPEI_{90d} < -1$), normal (D_4 , $-1 < SPEI_{90d} < 1$), and wet (D_5 , $SPEI_{90d} > 1$)⁷⁰. Secondly, multiple thresholds of temperature (T_{q50} , T_{q60} , T_{q70} , and T_{q80}) and $SPEI_{90d}$ ($SPEI_{90d-q20}$, $SPEI_{90d-q30}$, $SPEI_{90d-q40}$, and $SPEI_{90d-q50}$) are used to define different severities of hot droughts: HD_1 ($T > T_{q80}$ & $SPEI_{90d} < SPEI_{90d-q20}$; most severe), HD_2 ($T > T_{q70}$ & $SPEI_{90d} < SPEI_{90d-q30}$), HD_3 ($T > T_{q60}$ & $SPEI_{90d} < SPEI_{90d-q40}$), HD_4 ($T > T_{q50}$ & $SPEI_{90d} < SPEI_{90d-q50}$; least severe)⁶⁹. The main workflow of dataset processing and analyses is shown in Supplementary Fig. 16. The sources of the datasets used in this study are listed in Supplementary Table 4.

Vegetation provides numerous ecosystem services, and here we focus primarily on its cooling effects. We quantified the differences in temperature and cooling effects between areas with high vegetation cover (e.g., $NDVI > NDVI_{Q90}$) and those with low vegetation cover (e.g., $NDVI < NDVI_{Q10}$), as an exploration of the differences in cooling effects associated with vegetation inequality (details method in Supplementary Text 1).

Data availability

Data used in this study are collected from the following sources: The NDVI product used here are publicly available at https://developers.google.com/earth-engine/datasets/catalog/MODIS_006_MOD13Q1; The climate variables and drought index used here are publicly available at https://developers.google.com/earth-engine/datasets/catalog/GRIDMET_DROUGHT and https://developers.google.com/earth-engine/datasets/catalog/IDAHO_EPSCOR_GRIDMET#description; The social-economic variables at census track (2014-2018-American Census Survey) used here are publicly available at <https://www.census.gov/geographies/mapping-files/time-series/geo/tiger-data.2018.html>; US urban area boundaries (2018 Global Urban Boundary) are available at <http://data.ess.tsinghua.edu.cn/>;

The landcover from National Land Cover Database (NLCD) are publicly available at https://developers.google.com/earth-engine/datasets/catalog/USGS_NLCD_RELEASES_2016_REL; The climate zones from the updated Köppen-Geiger Climate Map are publicly available at <https://www.nature.com/articles/sdata2018214>. All other data are described and cited in the methods or appendices.

Code availability

The code for estimating VPI is available at <https://code.earthengine.google.com/cb7c3e44d8eb286b654fb14511b5e823>.

Received: 30 April 2025; Accepted: 25 September 2025;

Published online: 08 April 2026

References

- Richards, D. R. et al. Global variation in contributions to human well-being from urban vegetation ecosystem services. *One Earth* **5**, 522–533 (2022).
- Lai, K. Y., Kumari, S., Gallacher, J., Webster, C. & Sarkar, C. Nexus between residential air pollution and physiological stress is moderated by greenness. *Nat. Cities* **1**, 225–237 (2024).
- Yan, C., Guo, Q., Li, H., Li, L. & Qiu, G. Y. Quantifying the cooling effect of urban vegetation by mobile traverse method: a local-scale urban heat island study in a subtropical megacity. *Build. Environ.* **169**, 106541 (2020).
- Ow, L. F. & Ghosh, S. Urban cities and road traffic noise: reduction through vegetation. *Appl. Acoust.* **120**, 15–20 (2017).
- Gascon, M. et al. Residential green spaces and mortality: a systematic review. *Environ. Int.* **86**, 60–67 (2016).
- Ritchie, H. & Roser, M. Urbanization. *Our World in Data* (2018).
- Russell, C. SDG 11. *BGjournal* **15**, 31–33 (2018).
- Jenerette, G. D., Harlan, S. L., Stefanov, W. L. & Martin, C. A. Ecosystem services and urban heat riskscape moderation: water, green spaces, and social inequality in Phoenix, USA. *Ecol. Appl.* **21**, 2637–2651 (2011).
- McDonald, R. I. et al. The tree cover and temperature disparity in US urbanized areas: Quantifying the association with income across 5,723 communities. *PLoS ONE* **16**, e0249715 (2021).
- Nesbitt, L., Meitner, M. J., Girling, C., Sheppard, S. R. & Lu, Y. Who has access to urban vegetation? A spatial analysis of distributional green equity in 10 US cities. *Landsc. Urban Plan.* **181**, 51–79 (2019).
- Chen, B. et al. Contrasting inequality in human exposure to greenspace between cities of Global North and Global South. *Nat. Commun.* **13**, 1–9 (2022).
- Lin, J., Wang, Q. & Li, X. Socioeconomic and spatial inequalities of street tree abundance, species diversity, and size structure in New York City. *Landsc. Urban Plan.* **206**, 103992 (2021).
- Mohai, P., Pellow, D. & Roberts, J. T. Environmental Justice. *Annu. Rev. Environ. Resour.* **34**, 405–430 (2009).
- Abel, C. et al. The human–environment nexus and vegetation–rainfall sensitivity in tropical drylands. *Nat. Sustainability* **4**, 25–32 (2021).
- Swain, D. L. et al. The extraordinary California drought of 2013/2014: Character, context, and the role of climate change. *Bull. Am. Meteorol. Soc.* **95**, S3 (2014).
- Mini, C., Hogue, T. & Pincetl, S. Estimation of residential outdoor water use in Los Angeles, California. *Landsc. Urban Plan.* **127**, 124–135 (2014).
- Tuholske, C. et al. Global urban population exposure to extreme heat. *Proc. Natl. Acad. Sci.* **118**, e2024792118 (2021).
- Nesbitt, L., Meitner, M. J., Sheppard, S. R. & Girling, C. The dimensions of urban green equity: a framework for analysis. *Urban Forestry Urban Green.* **34**, 240–248 (2018).
- Schell, C. J. et al. The ecological and evolutionary consequences of systemic racism in urban environments. *Science* **369**, eaay4497 (2020).
- Guo, J. et al. How Extreme Events in China Would Be Affected by Global Warming—Insights From a Bias-Corrected CMIP6 Ensemble. *Earth's Future* **11**, e2022EF003347 (2023).
- Deepa, R., Kumar, V. & Sundaram, S. A systematic review of regional and global climate extremes in CMIP6 models under shared socio-economic pathways. *ThApC* **155**, 2523–2543 (2024).
- Wang, T., Tu, X., Singh, V. P., Chen, X. & Lin, K. Global data assessment and analysis of drought characteristics based on CMIP6. *J. Hydrol.* **596**, 126091 (2021).
- Trenberth, K. E. et al. Global warming and changes in drought. *Nat. Clim. Change* **4**, 17–22 (2014).
- Zscheischler, J. et al. Future climate risk from compound events. *Nat. Clim. Change* **8**, 469–477 (2018).
- Martin, A. J. F. & Conway, T. M. Using the Gini Index to quantify urban green inequality: A systematic review and recommended reporting standards. *Landsc. Urban Plan.* **254**, 105231 (2025).
- Sitthiyot, T. & Holasut, K. A simple method for measuring inequality. *Palgrave Commun.* **6**, 112 (2020).
- Britannica, T. E. o. E. *Sun Belt region, United States*, <https://www.britannica.com/place/Sun-Belt>.
- Mazdiyasi, O. & Aghakouchak, A. Substantial increase in concurrent droughts and heatwaves in the United States. *Proc. Natl. Acad. Sci.* **112**, 11484–11489 (2015).
- Volin, E. et al. Assessing macro-scale patterns in urban tree canopy and inequality. *Urban Forestry Urban Green.* **55**, 126818 (2020).
- Wu, S., Chen, B., Webster, C., Xu, B. & Gong, P. Improved equality of human exposure to greenspace in the 21st century urbanization. *Nat. Commun.* **14**, 6460 (2023).
- Gao, M. et al. Three-dimensional change in temperature sensitivity of northern vegetation phenology. *Glob. Change Biol.* **26**, 5189–5201 (2020).
- Bachelet, D., Neilson, R. P., Lenihan, J. M. & Drapek, R. J. Climate change effects on vegetation distribution and carbon budget in the United States. *Ecosystems* **4**, 164–185 (2001).
- Jia, W., Zhao, S. & Liu, S. Vegetation growth enhancement in urban environments of the Conterminous United States. *Glob. Change Biol.* **24**, 4084–4094 (2018).
- Rachunok, B. & Fletcher, S. Socio-hydrological drought impacts on urban water affordability. *Nat. Water* **1**, 83–94 (2023).
- Byers, E. A., Coxon, G., Freer, J. & Hall, J. W. Drought and climate change impacts on cooling water shortages and electricity prices in Great Britain. *Nat. Commun.* **11**, 2239 (2020).
- Mini, C., Hogue, T. S. & Pincetl, S. Patterns and controlling factors of residential water use in Los Angeles, California. *Water Policy* **16**, 1054–1069 (2014).
- Tschumi, E., Lienert, S., van der Wiel, K., Joos, F. & Zscheischler, J. The effects of varying drought-heat signatures on terrestrial carbon dynamics and vegetation composition. *Biogeosciences* **19**, 1979–1993 (2022).
- Neier, T. The green divide: A spatial analysis of segregation-based environmental inequality in Vienna. *Ecol. Econ.* **213**, 107949 (2023).
- Dong, C. et al. Drought-vulnerable vegetation increases exposure of disadvantaged populations to heatwaves under global warming: A case study from Los Angeles. *Sustain. Cities Soc.* **93**, 104488 (2023).
- Rocha, A. D. et al. Unprivileged groups are less served by green cooling services in major European urban areas. *Nat. Cities* **1**, 424–435 (2024).
- Wang, J. et al. Long-term exposure to residential greenness and decreased risk of depression and anxiety. *Nat. Ment. Health* **2**, 525–534 (2024).
- Liu, Z. et al. Green space exposure on depression and anxiety outcomes: A meta-analysis. *Environ. Res.* **231**, 116303 (2023).
- Kim, H., Lee, D.-K. & Sung, S. Effect of Urban Green Spaces and Flooded Area Type on Flooding Probability. *Sustainability* **8**, 134 (2016).

44. Jendritzky, G., de Dear, R. & Havenith, G. UTCI—Why another thermal index?. *Int. J. Biometeorol.* **56**, 421–428 (2012).
45. Yang, Z. et al. GloUTCI-M: a global monthly 1 km Universal Thermal Climate Index dataset from 2000 to 2022. *Earth Syst. Sci. Data* **16**, 2407–2424 (2024).
46. Gong, P. et al. Annual maps of global artificial impervious area (GAIA) between 1985 and 2018. *Remote Sens. Environ.* **236**, 111510 (2020).
47. Sun, L., Chen, J., Li, Q. & Huang, D. Dramatic uneven urbanization of large cities throughout the world in recent decades. *Nat. Commun.* **11**, 1–9 (2020).
48. Glaeser, E. L. & Tobio, K. The Rise of the Sunbelt. *South. Econ. J.* **74**, 609–643 (2008).
49. Beck, H. E. et al. Present and future Köppen-Geiger climate classification maps at 1-km resolution. *Sci. Data* **5**, 180214 (2018).
50. Hsu, A., Sheriff, G., Chakraborty, T. & Many, D. Disproportionate exposure to urban heat island intensity across major US cities. *Nat. Commun.* **12**, 2721 (2021).
51. Abatzoglou, J. T. Development of gridded surface meteorological data for ecological applications and modelling. *Int. J. Climatol.* **33**, 121–131 (2013).
52. Nanzad, L. et al. NDVI anomaly for drought monitoring and its correlation with climate factors over Mongolia from 2000 to 2016. *J. Arid. Environ.* **164**, 69–77 (2019).
53. Theil, H. A rank-invariant method of linear and polynomial regression analysis. *Indagationes Mathematicae* **12**, 173 (1950).
54. Panigrahi, S., Verma, K. & Tripathi, P. 12 - Review of MODIS EVI and NDVI data for data mining applications. in *Data Deduplication Approaches* (eds. Thwel, T. T. & Sinha, G. R.) 231–253 (Academic Press, 2021). <https://doi.org/10.1016/B978-0-12-823395-5.00018-5>.
55. Spotswood, E. N. et al. Nature inequity and higher COVID-19 case rates in less-green neighbourhoods in the United States. *Nat. Sustainability* **4**, 1092–1098 (2021).
56. Pettorelli, N. et al. Using the satellite-derived NDVI to assess ecological responses to environmental change. *Trends Ecol. Evol.* **20**, 503–510 (2005).
57. Gigliarano, C., Nowak, D. & Mosler, K. A polarization index for overlapping groups. *Rev. Income Wealth* **65**, 712–735 (2019).
58. Swart, J. in *No Poverty* 1–13 (Springer, 2020).
59. Esteban, J.-M. & Ray, D. On the measurement of polarization. *Econometrica: J. Econometric Soc.* **62**, 819–851 (1994).
60. Ravallion, M. Global poverty and inequality: a review of the evidence. No. 4623 (2008).
61. Burkhauser, R. V., Feng, S. & Jenkins, S. P. Using the P90/P10 index to measure US inequality trends with Current Population Survey data: a view from inside the Census Bureau vaults. *Rev. Income Wealth* **55**, 166–185 (2009).
62. Daly, M. C. & Valletta, R. G. Inequality and poverty in United States: the effects of rising dispersion of men's earnings and changing family behaviour. *Economica* **73**, 75–98 (2006).
63. Alexander, C. Normalised difference spectral indices and urban land cover as indicators of land surface temperature (LST). *Int. J. Appl. Earth Observation Geoinf.* **86**, 102013 (2020).
64. Gastwirth, J. L. The estimation of the Lorenz curve and Gini index. *Rev. Econom. Statistics* **54**, 306–316 (1972).
65. Wang, Y. Q. & Tsui, K. Y. Polarization orderings and new classes of polarization indices. *J. Public Economic Theory* **2**, 349–363 (2000).
66. Mann, H. Non-parametric tests against trend. *Econometrica* **13**, 245–259 (1945).
67. Peel, M. C., Finlayson, B. L. & McMahon, T. A. Updated world map of the Köppen-Geiger climate classification. *Hydrol. Earth Syst. Sci.* **11**, 1633–1644 (2007).
68. Auret, L. & Aldrich, C. Interpretation of nonlinear relationships between process variables by use of random forests. *Miner. Eng.* **35**, 27–42 (2012).
69. Feng, S. et al. A database for characteristics and variations of global compound dry and hot events. *Weather Clim. Extremes* **30**, 100299 (2020).
70. Wang, L., Chen, W., Zhou, W. & Huang, G. Understanding and detecting super-extreme droughts in Southwest China through an integrated approach and index. *Q. J. R. Meteorol. Soc.* **142**, 529–535 (2016).

Acknowledgements

The authors acknowledge the financial support from the National Key Research and Development Program of China (Grant No. 2023YFF1303600), the National Natural Science Foundation of China (Grants No. 42471150), the Guangdong Basic and Applied Basic Research Foundation (Grants No. 2023A1515030122), and the US Department of the Interior Southwest Climate Adaptation Science Center.

Author contributions

C.D. coordinated the project. Y.Y. and C.D. conceived the research and wrote the first draft of the paper. Y.Y. conducted the analyses. All authors (Y.Y., C.D., J.G. Z.L., K.L., X.C., D.L. and G.M.) contributed to the results assessment and interpretation, and the writing of the paper.

Competing interests

The authors declare no competing interests.

Additional information

Supplementary information The online version contains supplementary material available at <https://doi.org/10.1038/s44432-025-00001-1>.

Correspondence and requests for materials should be addressed to Chunyu Dong.

Reprints and permissions information is available at <http://www.nature.com/reprints>

Publisher's note Springer Nature remains neutral with regard to jurisdictional claims in published maps and institutional affiliations.

Open Access This article is licensed under a Creative Commons Attribution 4.0 International License, which permits use, sharing, adaptation, distribution and reproduction in any medium or format, as long as you give appropriate credit to the original author(s) and the source, provide a link to the Creative Commons licence, and indicate if changes were made. The images or other third party material in this article are included in the article's Creative Commons licence, unless indicated otherwise in a credit line to the material. If material is not included in the article's Creative Commons licence and your intended use is not permitted by statutory regulation or exceeds the permitted use, you will need to obtain permission directly from the copyright holder. To view a copy of this licence, visit <http://creativecommons.org/licenses/by/4.0/>.

© The Author(s) 2026